

Investigation of the two-way shape memory effect in [001]-oriented Co₃₅Ni₃₅Al₃₀ single crystals

Anna Eftifeeva, Elena Panchenko, Yuriy Chumlyakov, and Hans J. Maier

Citation: [AIP Conference Proceedings](#) **1698**, 030002 (2016); doi: 10.1063/1.4937824

View online: <http://dx.doi.org/10.1063/1.4937824>

View Table of Contents: <http://scitation.aip.org/content/aip/proceeding/aipcp/1698?ver=pdfcov>

Published by the [AIP Publishing](#)

Articles you may be interested in

[Role of B19' martensite deformation in stabilizing two-way shape memory behavior in NiTi](#)

J. Appl. Phys. **112**, 093510 (2012); 10.1063/1.4764313

[Two-way indent depth recovery in a NiTi shape memory alloy](#)

Appl. Phys. Lett. **88**, 131904 (2006); 10.1063/1.2189201

[Magnetic field-controlled two-way shape memory in CoNiGa single crystals](#)

Appl. Phys. Lett. **84**, 3594 (2004); 10.1063/1.1737481

[Stress-free two-way thermoelastic shape memory and field-enhanced strain in Ni₅₂Mn₂₄Ga₂₄ single crystals](#)

Appl. Phys. Lett. **77**, 3245 (2000); 10.1063/1.1325388

[Simple device for measuring the two-way shape memory effect](#)

Rev. Sci. Instrum. **55**, 114 (1984); 10.1063/1.1137582

Investigation of the Two-Way Shape Memory Effect in [001]-Oriented $\text{Co}_{35}\text{Ni}_{35}\text{Al}_{30}$ Single Crystals

Anna Eftifeeva^{1, a)}, Elena Panchenko¹, Yuriy Chumlyakov¹ and Hans J. Maier²

¹National Research Tomsk State University, Lenina Str., 36, Tomsk 634050, Russia
²Institut für Werkstoffkunde, Leibniz Universität Hannover, 30823 Garbsen, Germany

^{a)}Corresponding author: anna_eftifeeva@rambler.ru

Abstract. For the first time, a study of the two-way shape memory effect (the TWSME) for the quenched and aged at 673 K for 0.5 h [001]-oriented $\text{Co}_{35}\text{Ni}_{35}\text{Al}_{30}$ single crystals in compression was carried out. In the quenched CoNiAl crystals, the TWSME with a reversible strain of $(-3.1 \pm 0.3) \%$ was induced by training procedure in the superelasticity temperature range. The physical reason of the TWSME is the creation of internal stress fields due to the formation of dislocations next to γ -phase particles, and an interface between the B2-matrix and the γ -phase in the quenched crystals. It was experimentally shown that aging at 673 K for 0.5 h under a compressive stress of 100 MPa along the [110] direction creates the conditions necessary for observing the TWSME, without additional training with a reversible strain of $(+2.2 \pm 0.3) \%$. The conditions for observing the TWSME are determined by the action of the internal stress fields of 25 MPa created by the oriented arrangement of the dispersed particles in the stress-assisted aged crystals. The TWSME is not observed in the stress-free aged crystals with non-oriented precipitation of particles, both before and after training.

INTRODUCTION

Ferromagnetic CoNiAl alloys are the most promising materials undergoing the thermoelastic B2-L1₀ (B2 – bcc ordered phase, L1₀ – tetragonal martensite on the basis of the fct-lattice) martensitic transformation (MT) across a wide temperature range, from 200 K to 573 K. The shape and size of CoNiAl single crystals can be reversibly changed by the action of temperature (i.e. the shape memory effect (the SME)), mechanical stress (the superelasticity (the SE) response), and applied magnetic fields (the magnetic SME (the MSME)) [1-6]. It has been shown that CoNiAl single crystals oriented along the [001] direction demonstrate a high cyclic stability of the SE response, and a magnetically induced strain of 3.3 % under the action of both mechanical stress and magnetic fields [4,7]. These materials have the potential to be used as actuators, sensors and damping devices for various applications in the automobile and aerospace industries. The practical application of CoNiAl alloys can be extended by creating the necessary conditions for observing the TWSME. This unique functional property is the ability of the alloy, without external stress, to have spontaneous shape recovery induced during thermal cycling through a temperature range of reverse and forward transformations.

The TWSME can be induced under certain conditions (e.g. a special thermomechanical treatment and/or training), if the internal stress fields are present in the materials. The internal stress fields determine a selection of martensite variants at cooling and at an external applied stress of $|\sigma|=0\div 1$ MPa. The TWSME makes it possible to increase the transformation accuracy, or simplify the design of the devices, and also to reduce the number of component parts to break. It has been shown that the TWSME can be observed by oriented growth of the dispersed particles in the stress-assisted aged CoNiAl crystals oriented along the [011] and [123] directions [2,3]. However, no systematic study of the TWSME in quenched and aged CoNiAl single crystals oriented along the [001] direction has been performed yet. The choice of the [001] orientation for this study is predicated on the following reasons. First, theoretical calculations show that the maximum lattice strain along the [001] direction at the B2-L1₀ MT in compression is equal to -4.6 %. Secondly, in the crystals oriented along the [001] direction, the dislocation slip is suppressed in the high-temperature B2-phase (i.e. the Schmid factor equals to zero 0 for the $\langle 001 \rangle \{110\}$ slip system). This leads to high strength of austenite, the emergence of high-temperature SE at $T > 373$ K, and to high cyclic stability of the functional properties in [001]-oriented CoNiAl single crystals [4]. Based on these factors, the purpose of this work is to elucidate the conditions for observing the TWSME in

$\text{Co}_{35}\text{Ni}_{35}\text{Al}_{30}$ single crystals oriented along the [001] direction, which have been quenched and aged at 673 K for 0.5 h.

MATERIALS AND METHODS

Single crystals of $\text{Co}_{35}\text{Ni}_{35}\text{Al}_{30}$ (at. %) alloy were grown by the Bridgman technique in the atmosphere of an inert gas. The samples' orientation was verified with a DRON-3 X-ray diffractometer accurate to within $\pm 3^\circ$. The samples were cut in the shape of parallelepipeds along the [001] direction with the planes of sides as (110) and $(1\bar{1}0)$. Then, the samples were annealed at 1613 K for 8.5 h and were quenched in water of room temperature. These samples were aged at 673 K for 0.5 h in a free state and under a compressive stress of 100 MPa along the [110] direction in a vacuum chamber. We tried to exclude the difference of thermomechanical treatment for the stress-free and stress-assisted aged samples. The aging under stress applied along the [110] direction was selected to create nanocomposites with the oriented arrangement of the particles. After aging, the samples were cut out to the size $(3 \times 3 \times 6) \text{ mm}^3$ with a deformation axis along the [001] direction. They were ground and polished in 210 ml of an electrolytic solution $\text{H}_3\text{PO}_4 + 25 \text{ ml Cr}_2\text{O}_3$ at 293 K, $U = 20 \text{ V}$. Mechanical tests were carried out using a specially designed apparatus for measuring the SME during cooling/heating under constant stress with an output strain-temperature response $\epsilon(T)$ on the computer, and on InstronVHS 5969 at a rate of $\dot{\epsilon} = 10^{-3} \text{ 1/s}$. The microstructures of the samples were examined by transmission electron microscopy (TEM) using a JEOL 2010 operated at a nominal accelerating voltage of 200 kV. The foil for electron microscopic studies had a diameter of 3 mm and a thickness of 0.1 μm .

EXPERIMENT

The quenching from 1613 K leads to the two-phase state – the large γ -phase particles precipitate in the B2-matrix. These particles possess an fcc-structure, do not undergo the B2- L1_0 MT, and improve plasticity of ferromagnetic CoNiAl alloys [5]. The average volume fraction of the γ -phase in the samples is $f \sim 2 \%$ (Fig. 1).

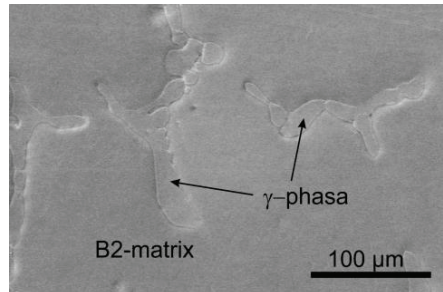


FIGURE 1. Scanning electron microscope (SEM) image of the microstructure of the quenched CoNiAl single crystal, consisting of the B2-matrix with the dispersed γ -phase

Electron microscopic studies of $\text{Co}_{35}\text{Ni}_{35}\text{Al}_{30}$ crystals show that nanoscale particles as small as 30 nm were observed after aging at 673 K for 0.5 h in the B2-phase (Fig. 2). Analysis of the published data shows that aging at 673 K gives rise to the precipitation of a few different types of particles, such as needle-like ϵ -Co particles with a hcp-lattice elongated along the near $\sim \langle 111 \rangle_{\text{B2}}$ direction (a ratio of length to thickness of ~ 9) and spherical particles, which can have a superstructure of either Ni_5Al_3 or L2_1 type [8-9]. Figure 2 (a) shows the bright-field image of B2-austenite with characteristic tweed contrast for the stress-free aged crystals, and the dark-field image taken from the reflection of nanoscale particles of size 5-10 nm. However, the microstructure of the stress-free and stress-assisted aged $\text{Co}_{35}\text{Ni}_{35}\text{Al}_{30}$ crystals requires further research.

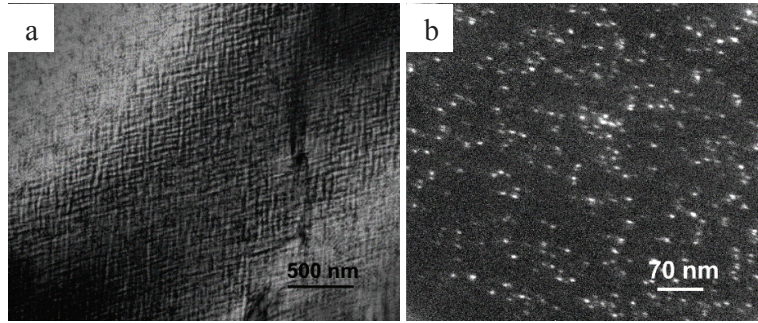


FIGURE 2. Bright-field image of B2-austenite with characteristic tweed contrast of the stress-free aged at 673 K for 0.5 h $\text{Co}_{35}\text{Ni}_{35}\text{Al}_{30}$ single crystals (a); the dark-field image from the reflection of the nanoscale particles of stress-assisted aged at 673 K for 0.5 h $\text{Co}_{35}\text{Ni}_{35}\text{Al}_{30}$ single crystals (b)

Figures 3 and 4 show strain-temperature curves $\epsilon(T)$ as a result of the cooling/heating under the action of various external compressive stress ($|\sigma| = 1\div 250$ MPa) for the quenched, stress-free and stress-assisted aged at 673 K for 0.5 h $\text{Co}_{35}\text{Ni}_{35}\text{Al}_{30}$ single crystals oriented along the [001] direction. The dependence of the martensite start initial temperature on the external applied stress $\sigma(T)$ for $\text{Co}_{35}\text{Ni}_{35}\text{Al}_{30}$ single crystals is presented in Fig. 5.

The TWSME (change of the sample size at a minimum external stress of $|\sigma| = 0\div 1$ MPa, which is necessary to secure the sample in the grips of the machine) is not observed without an additional training procedure in the quenched $\text{Co}_{35}\text{Ni}_{35}\text{Al}_{30}$ single crystals. In [4], the authors showed that the TWSME can be induced by thermal cycling through an interval of the B2-L1₀ MT under action of a constant external stress of 40 MPa in quenched crystals. However, this training is not effective: the TWSME is realized with the value of reversible strain (the TWSME strain) of 1 % [4]. Therefore, the training procedure in the SE response was used in this work to create conditions for observing the TWSME: 100 cycles of loading/unloading at room temperature ($T = 293$ K) with the maximum value of reversible strain of (6.0 ± 0.3) %. This training creates the internal stress fields necessary for the realization of the TWSME due to the formation of dislocations next to the γ -phase particles, and an interface between the B2-matrix and the γ -phase, as is shown elsewhere [10]. In the quenched crystals, the TWSME strain is $\epsilon_{\text{TWSME}} = (-3.1 \pm 0.3)$ % after the training procedure in the SE temperature range.

The martensite start temperature M_s increases linearly with the growth of external stresses, according to the Clausius-Clapeyron relationship [6]: $d\sigma/dT = -\Delta H/(\epsilon T_0)$, where ΔH is the change of enthalpy associated with the forward transformation, and ϵ is the transformation strain. The coefficient of the $\sigma(T)$ curve slope is $\alpha_1 = d\sigma/dT = 2.0$ MPa/K (see curve marked 1 on Fig. 5). During the cooling/heating cycle under an external stress of 20 MPa, the reversible strain (the SME strain) amounts to a maximum value of $\epsilon_{\text{SME}} = (-4.2 \pm 0.3)$ % (Fig. 3). The experimental values of the SME are close to the theoretical lattice strain for the [001] direction at the B2-L1₀ MT of $\epsilon_{\text{t0}} \sim -4.6$ %. Therefore, the totally oriented martensite is formed at cooling under the action of $|\sigma| = 20$ MPa and disappears during heating at the reverse transformation. The value of temperature hysteresis ΔT , which characterizes the energy dissipation at MT, decreases with increasing external applied stress (Fig. 3). The value of ΔT is determined as the difference between the temperature of the forward and reverse MT in the middle of the loop $\epsilon(T)$.

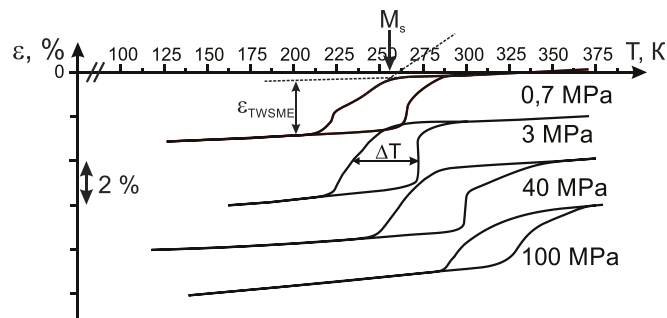


FIGURE 3. Strain-temperature response $\epsilon(T)$ of quenched [001]-oriented $\text{Co}_{35}\text{Ni}_{35}\text{Al}_{30}$ single crystals during cooling/heating, under the action of various external compressive stresses

The TWSME was not observed in the stress-free aged [001]-oriented crystals: during the cooling process, a self-accommodated microstructure of the L1₀-martensite is formed in the stress range 1-10 MPa, the dimensions and shape of the sample are unchanged. The transformation strain increases with the external applied stress and the maximum SME strain of $\epsilon_{\text{SME}} = (-3.8 \pm 0.3) \%$ is observed at 50 MPa. The SME strain is constant when the stress increases $|\sigma| \geq 50$ MPa (Fig. 4 (a)). The precipitation of dispersed particles leads to a reduction of the ϵ_{SME} in stress-free aged crystals compared to quenched crystals. This phenomenon is related to the fact that the dispersed particles do not undergo the MT, the volume fraction of the material, in which the MT occurs, decreases. The maximum value of theoretical lattice strain is $\epsilon_{\text{tr0}}' = \epsilon_{\text{tr0}}(1-f) = -3.7 \%$ in the aged [001]-oriented crystals ($f = 20\%$ is the average volume fraction of the dispersed particles precipitated during aging at 673 K for 0.5 h).

The experimental value of the maximum reversible strain in the stress-free aged crystals is close to the theoretical calculated value of transformation strain. It should be pointed out that, to achieve the maximum value of the reversible strain in the aged crystals, the stresses are required to be 2.5 times larger compared to the quenched crystals. The martensite start temperature M_s' increases with the growth of the external stresses with the coefficient $\alpha_2 = 2.4$ MPa/K (Fig. 5, curve 2), and shifts toward lower temperatures compared to the quenched crystals. The increase of external applied stresses is accompanied by a decrease of the temperature hysteresis ΔT (Fig. 4 (a)).

It has been experimentally shown that in the stress-assisted aged $\text{Co}_{35}\text{Ni}_{35}\text{Al}_{30}$ single crystals, the conditions for observing the TWSME have been created without additional training. The maximum TWSME strain of $\epsilon_{\text{TWSME}} = (+2.2 \pm 0.3) \%$ is observed at $|\sigma| = 1$ MPa. The value of reversible strain decreases with the growth of stress from $1 \div 20$ MPa and changes sign to $\epsilon_{\text{SME}} = (-1.2 \pm 0.3) \%$ at $|\sigma| = 30$ MPa (Fig. 4 (b)). The value of ϵ_{SME} is constant under the action of a stress of $|\sigma| \geq 30$ MPa. The transformation strain equals to zero at $|\sigma| = 25$ MPa, consequently, a value of 25 MPa can be taken as the value of the internal stress fields $|\langle \sigma_G \rangle|$. Thus, in the stress-assisted aged $\text{Co}_{35}\text{Ni}_{35}\text{Al}_{30}$ single crystals, if $|\sigma| \leq 25$ MPa, the internal stress fields lead to growth of the martensite variants expandable size of the sample along the [001] direction. When the external compressive stress becomes higher than the internal stress (i.e. $|\sigma| \geq 25$ MPa), during cooling the martensite variants grow oriented to the external compressive stress, and the size of the sample decreases. According to the Clausius-Clapeyron relationship, the temperature M_s' should increase with growth of the external stress. This dependence is realized at $|\sigma| \geq 25$ MPa with the coefficient $\alpha_3 = 2.0$ MPa/K (Fig. 5, curve 3).

However, the temperature M_s' decreases with the coefficient $\alpha_3' = -0.6$ MPa/K under the action of an external compressive stress of $|\sigma| \leq 25$ MPa (curve marked 3' on Fig. 5). The internal stress fields lead to an increase of the sample size along the [001] direction, consequently, they are tensile. The internal and external stresses generate the different martensite variants. Consequently, an increase of external compressive stresses leads to a decrease of the effective stresses in crystal $|\sigma_{\text{eff}}| = |\langle \sigma_G \rangle - \sigma|$. The effective stresses contribute to the growth of the martensite variant, which increases the size of the sample along the [001] direction. The temperature M_s' decreases with application of opposing stresses from $1 \div 25$ MPa (curve marked 3' on Fig. 5) and the $\sigma_{\text{eff}}(T)$ dependence corresponds to the Clausius-Clapeyron relationship [6] (see inset on Fig. 5). The value of ΔT decreases with the growth of the external stress of $|\sigma| \geq 100$ MPa (Fig. 4 (b)).

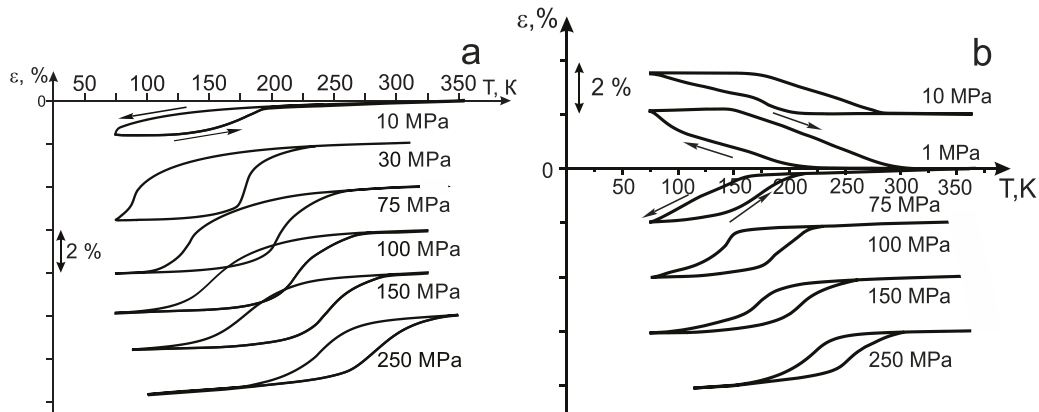


FIGURE 4. Strain-temperature response $\epsilon(T)$ of the stress-free (a) and stress-assisted (b) aged at 673 K for 0.5 h [001]-oriented $\text{Co}_{35}\text{Ni}_{35}\text{Al}_{30}$ single crystals during cooling/heating under the action of various external compressive stresses

Thus, the training and precipitation of particles do not lead to the observation of the TWSME in the stress-free situation compared to the quenched and stress-assisted aged single crystals of CoNiAl. The stress-assisted aging crystals have high external stresses for stress-induced MT, compared to the stress-free aged single crystals at the same temperature, as shown in Fig. 5. The presence of the internal stress $|\langle\sigma_G\rangle| \sim 25$ MPa prevents compression of the sample and leads to a decrease in the effective compressive stresses $|\sigma_{\text{eff}}| = |\langle\sigma_G\rangle - \sigma|$ in the stress-assisted aged crystals (curve marked 4 on Fig. 5).

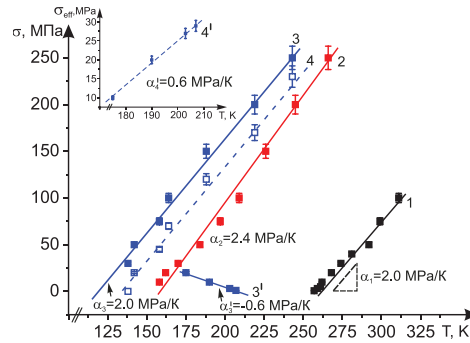


FIGURE 5. The dependence of martensite start temperature M_s' on the external compressive stress $\sigma(T)$ of the quenched (curve 1), stress-free (curve 2) and stress-assisted (curves 3, 3', 4 and 4') aged at 673 K for 0.5 h [001]-oriented $\text{Co}_{35}\text{Ni}_{35}\text{Al}_{30}$ single crystals

A check of the TWSME stability was carried out in the stress-assisted aged at 673 K for 0.5 h crystals. The thermal cycling through an interval of the forward and reverse B2-L1₀ MT under the action of the external opposing stresses of 250 MPa was carried out, and then the TWSME was investigated (Fig. 6). Figure 7 presents the dependence of strain and temperature hysteresis on the number of loading/unloading cycles. Such a thermal cycling does not lead to suppression of the TWSME (Figs. 6 and 7); change of the martensite start temperature M_s' is absent. However, the value of the TWSME decreases by 0.4 % after the thermal cycling in the conditions of the opposing stresses (Figs. 6 and 7: curve marked 1).

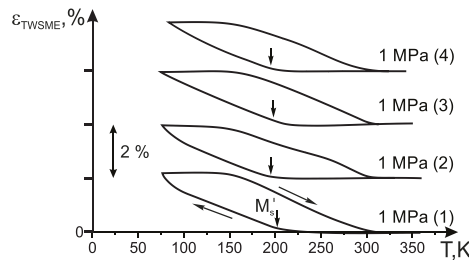


FIGURE 6. Strain-temperature response $\epsilon(T)$ of the stress-assisted aged at 673 K for 0.5 h [001]-oriented $\text{Co}_{35}\text{Ni}_{35}\text{Al}_{30}$ single crystals during cooling/heating under the action of an external compressive stress of $|\sigma| = 1$ MPa

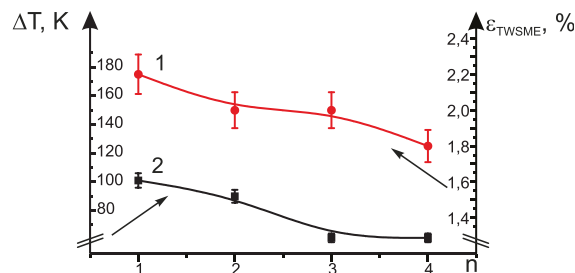


FIGURE 7. The dependence of strain (curve 1) and temperature hysteresis (curve 2) on the number of cycles $n(\epsilon)$ and $n(\Delta T)$, respectively of the stress-assisted aged at 673 K for 0.5 h [001]-oriented $\text{Co}_{35}\text{Ni}_{35}\text{Al}_{30}$ single crystals

CONCLUSIONS

1. It was experimentally shown that the two-way shape memory effect with reversible strain of $\varepsilon_{\text{TWSME}} = (-3.1 \pm 0.3) \%$ was induced in quenched [001]-oriented $\text{Co}_{35}\text{Ni}_{35}\text{Al}_{30}$ (at. %) single crystals by the training procedure in the superelasticity response: 100 cycles of loading/unloading were carried out at room temperature ($T = 293 \text{ K}$) with a maximum value of reversible strain of $(6.0 \pm 0.3) \%$. The physical reason of the two-way shape memory effect is the creation of the internal stress fields due to the formation of dislocations next to γ -phase particles, and an interface between the B2-matrix and the γ -phase.

2. Neither the training procedure in the superelasticity response, nor the precipitation of particles leads to the observation of the two-way shape memory effect in the stress-free aged $\text{Co}_{35}\text{Ni}_{35}\text{Al}_{30}$ single crystals, because the aging at 673 K for 0.5 h leads to precipitation strengthening of the matrix, and the local internal stress fields relax in the material. The aging leads to a shift of the martensite interval temperature M_s' toward a lower temperature, and an increase of the stresses necessary to realize maximum transformation strain, 2.5 times larger, compared to quenched crystals.

3. For the first time we have shown experimentally that the stress-assisted aging at 673 K for 0.5 h along the [110] direction creates the conditions for observing the two-way shape memory effect with values of reversible strain of $\varepsilon_{\text{TWSME}} = (+2.2 \pm 0.3) \%$ along the [001] direction. The spontaneous increase of the sample's linear dimension along the [001] direction at cooling is caused by the action of the internal stress fields $|\langle \sigma_G \rangle| \sim 25 \text{ MPa}$. They lead to growth of the oriented martensite during cooling of the stress-assisted aged sample at an external stress of 0–1 MPa.

4. The thermal cycling through an interval of the forward and reverse B2-L1₀ martensitic transformation under the action of external opposing stresses of 250 MPa does not lead to suppression of the two-way shape memory effect in the stress-assisted aged $\text{Co}_{35}\text{Ni}_{35}\text{Al}_{30}$ single crystals.

ACKNOWLEDGEMENTS

The reported study was partially supported by the RFBR (Grant No. 13-03-98024) and “The Tomsk State University Academic D.I. Mendeleev Fund Program”.

REFERENCES

1. E. Yu. Panchenko, Yu. I. Chumlyakov, H. Maier, V. A. Kirillov and A. S. Kanafieva, *Russ. Phys. J.* **54**, 721-728 (2011).
2. E. Yu. Panchenko, Yu. I. Chumlyakov, H. Maier, A. S. Kanafieva and V. A. Kirillov, *Russ. Phys. J.* **55**, 1123-1131 (2013).
3. E. Panchenko, Y. Chumlyakov, A. Eftifeeva, H.J. Maier, *Scr. Mater.* **90-91**, 10-13 (2014).
4. J. Dadda, H. J. Maier, I. Karaman and Y. I. Chumlyakov, *Acta Mater.* **57**, 6123-6134 (2009).
5. Y. Tanaka, K. Oikawa, Y. Sutou, T. Omori, R. Kainuma and K. Ishida, *Mater. Sci. Eng. A* **438-440**, 1054-1060 (2006).
6. K. Otsuka, C. M. Wayman, *Shape memory materials* (Cambridge University Press, Cambridge, 1998), pp. 284.
7. H. Morito, K. Oikawa, A. Fujita, *Scr. Mater.* **63**, 379-382 (2010).
8. A. I. Valiullin, I. I. Kositsyna, S. V. Kositsyn, N. V. Kataeva, *Mater. Sci. Eng. A* **481-482**, 551-554 (2008).
9. B. Bartova, D. Schryvers, Z. Yang, S. Ignacovab, P. Sittnerb, *Scr. Mater.* **57**, 37-40 (2007).
10. R. F. Hamilton, H. Sehitoglu, C. Efstathiou, H. J. Maier, Y. Chumlyakov, *Acta Mater.* **54**, 587-599 (2006).